JCTC Journal of Chemical Theory and Computation

Article

pubs.acs.org/JCTC

Thermodynamic and Transport Properties of H_2O + NaCl from Polarizable Force Fields

Hao Jiang,[†] Zoltan Mester,[†] Othonas A. Moultos,[‡] Ioannis G. Economou,[‡] and Athanassios Z. Panagiotopoulos*,[†]

[†]Department of Chemical and Biological Engineering, Princeton University, Princeton, New Jersey 08544, United States

[‡]Chemical Engineering Program, Texas A&M University at Qatar, P.O. Box 23874, Doha, Qatar

Supporting Information

ABSTRACT: Molecular dynamics and Monte Carlo simulations were performed to obtain thermodynamic and transport properties of the binary H_2O + NaCl system using the polarizable force fields of Kiss and Baranyai (*J. Chem. Phys.* **2013**, *138*, 204507 and **2014**, *141*, 114501). In particular, liquid densities, electrolyte and crystal chemical potentials of NaCl, salt solubilities, mean ionic activity coefficients, vapor pressures, vapor−liquid interfacial tensions, and viscosities were obtained as functions of temperature, pressure, and salt concentration. We compared the performance of the polarizable force fields against fixed-point-charge (nonpolarizable) models. Most of the properties of interest are better represented by the polarizable models, which also remain physically realistic at elevated temperatures.

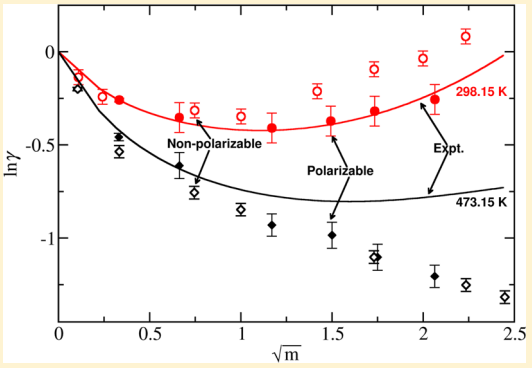

I. INTRODUCTION

Aqueous electrolyte solutions are widely present in industrial and biological processes; understanding the nature of such solutions is of great importance to geochemistry, biophysical chemistry, corrosion, and interplanetary science. Despite concerted research efforts over the past several decades, modeling of these solutions remains a challenge because of the complex, hydrogen-bonding character of the solvent and the strong Coulombic interactions resulting from the presence of the ions in solution.

Empirical approaches such as activity coefficient models[1] and cubic equations of state[2,3] are widely used to model electrolyte solutions. Nevertheless, such approaches cannot be extrapolated outside the range of available experimental data. Perturbation theory based models, such as the associated perturbed anisotropic chain theory and statistical associating fluid theory, have also been applied to the modeling of aqueous electrolyte solutions.[4−6] The hydrogen-bonding interactions of water molecules and the long-range electrostatic interactions of ions are approximately represented through Poisson−Boltzmann or integral equations. Temperature- or composition-dependent interaction parameters are often used, which limit the predictive power of these models.

Molecular simulation using transferable force-field models can provide reliable estimations for the properties of aqueous electrolyte solutions. The binary H_2O + NaCl mixture has been extensively investigated by molecular dynamics (MD) and Monte Carlo (MC) simulations using a variety of force fields. MD simulations were performed by Hummer et al.[7] and Brodholt[8] to study the effect of salt concentration on the structure of NaCl solution. The water models used in these simulations were SPC[9] and SPC/E,[10] respectively, and the Smith−Dang (SD)[11] force field was used for NaCl. Smith and co-workers[12−14] developed the osmotic ensemble Monte Carlo simulation method to calculate the chemical potentials of salts in solution. In ref 13, the NaCl chemical potential and solubility were obtained by osmotic ensemble Monte Carlo simulations, using the SPC/E and Joung−Cheatham[15] models to represent water and NaCl, respectively. Moučka et al.[16] examined 13 commonly used force fields of NaCl and SPC/E water with respect to their prediction of electrolyte chemical potential and NaCl solubility. In ref 17, the electrolyte and water chemical potentials for the H_2O + NaCl mixture were obtained for the Joung−Cheatham ion and SPC/E water models, and the Gibbs−Duhem consistency of the model combinations was confirmed. In the work of Mester and Panagiotopoulos,[18] a different approach for obtaining the chemical potentials of NaCl and water was proposed, based on gradual insertion of an ion pair into the solution and matching a low-concentration reference activity coefficient. In that work, the SPC/E,[10] TIP4Pew,[19] and Exp-6[20] water models were used, and SD,[11] Jouth−Cheatham (JC),[15] and Tosi−Fumi (TF)[21] force fields were used to represent the NaCl. Orozco et al.[22] conducted a comprehensive simulation study of thermodynamic and transport properties for the H_2O + NaCl system using several fixed-point-charge nonpolarizable water (SPC,[9] SPC/E,[10] semiflexible SPC/E,[23] and Exp-6[20]) and ion (SD,[11] JC,[15] and

Received: May 7, 2015
Published: July 7, 2015

DOI: 10.1021/acs.jctc.5b00421
J. Chem. Theory Comput. 2015, 11, 3802−3810

TF[21]) force fields. The vapor pressures, liquid densities, interfacial tensions, and viscosities were calculated as functions of temperature, pressure, and NaCl concentration. It was found that none of these nonpolarizable force field combinations simultaneously reproduce all properties of interest, which strongly motivates continuing investigations of improved force fields for aqueous electrolytes.

Introducing polarizability is a promising path to improve quantitative predictions of properties of aqueous electrolyte solutions. There are several possible approaches for the inclusion of polarizability in a classical force field: e.g., fluctuating charges, polarizable dipoles or multipoles, and Drude oscillators. In the fluctuating charge approach, the partial charges are dynamically changed with the local environment. Berne and co-workers[24] proposed force fields for water with fluctuating charges using the SPC[9] and TIP4P potentials.[25] Although the fluctuating charge approach is computationally efficient, the polarizability of the model has to be constrained on the molecular plane. Ponder and co-workers[26,27] developed the "AMOEBA" models based on polarizable atomic multipoles, but a recent calculation[28] shows that the water model underestimates the saturated liquid densities, overestimates the saturated vapor densities, and underpredicts the critical temperature by approximately 50 K. Paricaud et al.[29] developed a Gaussian charge polarizable model (GCP) for water by placing a point dipole at the center of mass of the TIP4P water molecule. The model accurately predicts dimer energies, saturated densities, vapor pressures, and the dielectric constant but requires complex evaluations of dipole−dipole interaction forces and energies. Chialvo et al.[30] recently demonstrated that the polarization of the GCP model can be represented through the Drude oscillator approach. In the Drude oscillator (or charge-on-spring) approach, a partial charge is attached to a particular interaction site. Such models were proposed by Yu and van Gunsteren[31] and Roux and co-workers,[32,33] who developed both four-site (SWM4) and six-site (SWM6) water models. Ion models (AH/SWM4-DP and AH/SWM4-NDP) that are compatible with the SWM4 water force field were also developed for alkali halide (AH) salts.[34,35] With the AH/SWM4-DP and AH/SWM4-NDP models, Neyt et al.[36] calculated the interfacial tensions and densities of the H_2O + NaCl mixture and concluded that the AH/SWM4 models are unable to reproduce the changes in surface tension with salt concentration. Moučka et al.[37] presented the first simulation study of the NaCl chemical potential using the SWM4-DP model for the mixture. Drude oscillator based polarizable water (BK3)[38] and ion (AH/BK3)[39] force fields were developed by Kiss and Baranyai. In an important recent study, Moučkaet al.[40] calculated the densities, electrolyte chemical potential, activity coefficients, and salt solubilities for the H_2O + NaCl mixture at 298.15 K using the AH/BK3, AH/SWM4-DP, and SPC/E+JC force fields. The BK3 set of polarizable force fields were shown to yield better agreement with experimental data compared with the AH/SWM4-DP models for the mean ionic activity coefficients and salt solubility. However, other thermodynamic and transport properties of the solution were not studied, and the quality of activity coefficient predictions at elevated temperatures, which is important for geophysical and carbon sequestration applications, was not examined.

In the present work, we obtain several key properties of the binary H_2O + NaCl mixture over a wide range of salt concentrations and temperatures, using the polarizable BK3 water and AH/BK3 NaCl force fields. The performance of the polarizable SWM4-NDP water and AH/SWM4-NDP NaCl force fields with respect to the prediction of vapor pressure was also studied. A broad range of different molecular simulation techniques were used that include MD and MC simulations in different statistical ensembles. The objective of the present study is to compare polarizable model combinations to previously developed nonpolarizable force fields with respect to liquid densities, electrolyte and crystal chemical potentials, NaCl solubilities, mean ionic activity coefficients, vapor pressures, vapor−liquid interfacial tensions, and viscosities. We also report the temperature effect on the mean ionic activity coefficients and chemical potentials of NaCl using the BK3 family of force fields.

This article is organized as follows: simulation details and methodology of the MD and MC calculations are given in subsections IIA and IIB, respectively. The BK3 force fields of water and NaCl are briefly described in subsection IIC. Results for liquid densities, electrolyte and crystal chemical potentials, salt solubilities, mean ionic activity coefficients, vapor pressures, vapor−liquid interfacial tensions, and viscosities are presented in section III. Finally, the main conclusions are summarized in section IV.

II. METHODS AND MODELS

A. Molecular Dynamics Simulations. Liquid densities, chemical potentials of NaCl, mean ionic activity coefficients, vapor−liquid interfacial tensions, and viscosities were obtained from MD simulations using the open-source GROMACS package,[41] modified by Kiss et al. to include the BK3 force fields.[42] Most of the MD simulations were performed in the isothermal−isobaric ensemble, while simulations in the canonical ensemble were carried out to obtain the vapor−liquid interfacial tensions. Nosé−Hoover[43] thermostat and Parrinello−Rahman[44] barostat, with coupling constants of 0.5 and 1.0 ps, respectively, were used to control the system temperature and pressure. For the isothermal−isobaric simulations, the systems were equilibrated for 2 ns followed by a production period of 10 ns. For canonical ensemble simulations, an equilibration period of 6 ns was performed to stabilize the vapor−liquid interface, and the production period was 8 ns. The integration time step of the equilibration periods was set to 1 fs, while the time step was set to 2 fs for the production period.

The number of H_2O molecules used in the MD simulations was 500, while the number of NaCl molecules varied according to the desired molality. Finite-size effects were tested by running larger systems (864 water molecules) for selected molalities and temperatures. Results for the larger systems agreed within statistical uncertainties with those of the base size. For simulations in the isothermal−isobaric ensemble, the cutoff distance was set to 9 Å, both for the Buckingham interaction and the real-space electrostatics, and the standard long-range correction of the Buckingham interaction was applied to the energy and pressure calculation. The long-range Coulombic interactions of Gaussian charges were efficiently handled by the particle-mesh Ewald (PME) method proposed by Kiss et al.;[42] the Fourier-spacing parameter of the PME summation was set to 0.12. The positions of the Drude particles were calculated by the modified "Always Stable Predictor-Corrector" method of Kolafa,[42,45] and the force on the Drude particle was relaxed to 0.05 kJ/(mol·nm). A typical isothermal−isobaric MD simulation took about 125 h to finish on a single 2.5 GHz intel IvyBridge core.

DOI: 10.1021/acs.jctc.5b00421
J. Chem. Theory Comput. 2015, 11, 3802−3810

The electrolyte chemical potential in solution (μ_{NaCl}) was obtained from the free energy change resulting from adding a cation−anion pair to the system following the methodology of Mester and Panagiotopoulos.[18] In the MD simulations, the interactions between the added ion pair and the rest of the system were controlled by a scaling parameter λ. The values of λ were (0,0.1,...,1) for Coulombic interactions and (0,0.02,...,0.1,0.2,...,1.0) for Buckingham interactions. The free energy was calculated using the Bennett's acceptance ratio method,[46] and the statistical uncertainties of the free energy were estimated by the bootstraping procedure of Mester and Panagiotopoulos,[18] and Paliwal and Shirts.[47] The mean ionic activity coefficient of NaCl (γ) can be related to the electrolyte chemical potential of NaCl (μ_{NaCl}) through the following equation:

$$\beta\mu_{NaCl} = \beta\mu^{\pm}_{NaCl} + 2\ln m + 2\ln\gamma \quad (1)$$

where m is the molality of the solution, and $\mu^{\pm}_{NaCl}$ is the Henry's law standard state chemical potential of salt. In order to calculate the mean ionic activity coefficient from eq 1, $\mu^{\pm}_{NaCl}$ must be obtained first. We calculated the electrolyte chemical potential of the system at 0.11 mol/kg (the lowest concentration studied), and set $\mu^{\pm}_{NaCl}$ so that the calculated γ at this concentration matches the mean activity coefficient calculated from Davies equation,[48] which is an empirical extension of the Debye−Hückel limiting law,

$$\ln\gamma = -A\left(\frac{\sqrt{m}}{1+\sqrt{m}} - 0.2m\right)\ln(10) \quad (2)$$

where A is given by

$$A = \frac{1.824\times 10^6}{(\epsilon T)^{3/2}} \quad (3)$$

and ϵ is the relative permittivity of the BK3 water model, which was obtained from the fluctuation of the total dipole moment of the simulation box. The values of relative permittivities can be found in the Supporting Information. The standard molar chemical potentials of Na^+ and Cl^- were taken from the NIST-JANAF thermochemical tables.[49]

To calculate the interfacial tensions, MD simulations in the canonical ensemble were performed in a tetragonal box of dimensions $L_x = L_y = 1/3L_z = 35$ Å. The cutoff distance was 13.5 Å, and no long-range corrections were applied to the Buckingham potential. To analyze the effect of cutoff distance on the interfacial tension calculation, the cutoff distance was increased to 15.0 Å in several simulations, and similar results were obtained, which indicates that the contribution of the Buckingham potential beyond the cutoff distance is negligible. The vapor−liquid interfacial tensions (σ) were determined from the diagonal stress tensor elements (P_{zz}, P_{xx}, and P_{yy}) through the following equation:[50,51]

$$\sigma = \frac{L_z}{2}[\langle P_{zz}\rangle - 0.5\times(\langle P_{xx}\rangle + \langle P_{yy}\rangle)] \quad (4)$$

Statistical uncertainties of interfacial tensions were obtained from block averages of a single run. The Green−Kubo relationships were used to calculate the shear viscosity (η):[52]

$$\eta(t) = \frac{V}{k_B T}\int_0^t \langle P_{\alpha\beta}(t_0)P_{\alpha\beta}(t_0+t)\rangle dt \quad (5)$$

where V is the volume of the simulation box, and $P_{\alpha\beta}$ denotes the off-diagonal element of the pressure tensor. The stress tensor elements were collected from the production period of MD simulations (with a time step of 1 fs). The angle brackets indicate an ensemble average over all time origins t_0. For improved statistics, the autocorrelation functions over all independent off-diagonal tensor elements P_{xy}, P_{xz}, and P_{yz} were averaged. Because of the rotational invariance, the equivalent $(P_{xx}-P_{yy})/2$ and $(P_{yy}-P_{zz})/2$ terms were also added. The viscosity at each state point and the respective statistical uncertainty were calculated from five independent simulations, each starting from a completely different initial configuration.

B. Monte Carlo Simulations. The Cassandra suite of MC codes[53] (beta release version), with our modification to include the BK3 force fields, was used to perform all MC simulations reported in this article. Gibbs-ensemble MC simulations were performed at constant volume and temperature[54,55] to obtain the vapor pressures of the binary H_2O + NaCl mixture. Since the interactions of polarizable models are not pairwise additive, a multiparticle move method, originally developed by Moučka et al.,[37] was used in the simulations to efficiently sample phase space. In the Gibbs ensemble simulations, all molecules in both vapor and liquid phases were displaced simultaneously in one step. The base system size was 256 water molecules, with the number of ions varying to obtain a desired molality. Finite-size effects were studied by doubling the system size at low and high molalities at 473.15 K, and the vapor pressures obtained were within statistical uncertainties of results obtained from the base system size. The cutoff distances for the Buckingham potential and real space electrostatic interactions were set to 9 Å, and standard long-range correction of the Buckingham potential was used. The long-range part of the electrostatic interactions was handled by Ewald summation as suggested in ref 56. The convergence parameter for the Ewald summation was about 0.3 $Å^{-1}$ depending on the size of the simulation box, and the number of wave vectors used for summation in the reciprocal space was about 600−700. The setting of the Ewald summation was chosen to achieve a relative accuracy of 10^{-4} in electrostatic energy. The forces on the Drude particles were calculated at every MC step, and the positions of Drude particles were determined by the following iteration:

$$\mathbf{r}_{iD}(n) = \mathbf{r}_{iD}(n-1) + \mathbf{F}_{iD}/k \quad (6)$$

where $r_{iD}(n)$ denotes the position of Drude particle of molecule i in step n of the iteration, F_{iD} is the force acting on the Drude particle, and k is the spring constant of the harmonic spring connecting the Drude particle. The iteration was terminated if the following condition was satisfied:

$$\max_{i=1\ldots N}|\mathbf{r}_{iD}(n) - \mathbf{r}_{iD}(n-1)| < 10^{-4}\ \text{nm} \quad (7)$$

A typical simulation run consisted of an equilibration period of 10 million steps followed by a production period of 10 million steps. The MC moves were multiparticle translations (constituting a fraction of 0.25 of total moves), multiparticle rotations (0.25), volume changes (0.1), and transfers of particles with configurational bias (0.4).[57] The volume change moves were performed in the standard way.[58] Since no salt is present in the vapor phase over the range of temperatures studied, the transfer probability of NaCl was set to zero. It is worth pointing out that setting the transfer probability of salt to zero is not an artificial constraint; interfacial MD simulations in

DOI: 10.1021/acs.jctc.5b00421
J. Chem. Theory Comput. 2015, 11, 3802−3810

long rectangular boxes demonstrate that no ions are present in the vapor phase even when the ions are given the freedom to move between phases.[51] A typical Gibbs-ensemble MC simulation took about 300 h using 16 2.6 GHz Intel Sandybridge cores. The statistical uncertainties of vapor pressures were calculated from block averages of a single run.

The chemical potential of NaCl in the solid phase (for the solubility calculations) was calculated from the Helmholtz free energy of the crystal. We employed the Einstein crystal method of Aragones et al.[59] The NaCl crystal density was first determined from standard isothermal−isobaric MC simulations. To control for system size effects, three isothermal−isobaric MC simulations using 512, 1000, and 1728 ions were performed at each temperature of interest to calculate the system density, and the crystal density was determined by extrapolating to infinite system size. A series of MC simulations in the canonical ensemble was then performed at the crystal density for the model under study to estimate the free energy difference between the system of interest and the Einstein crystal reference. For the estimation of free energy, a relatively large system (1000 ions) was used in the MC simulations, and the cutoff distance was set to 14 Å, as suggested by Aragones et al.[59] Standard single particle moves were performed to sample phase space. Systems were equilibrated for 500,000 steps followed by a production period of 1 million steps. Statistical uncertainties of the Helmholtz free energy were estimated from block averages. After the crystal chemical potential was obtained, the salt solubility was determined by finding the salt concentration where the electrolyte chemical potential equals the crystal chemical potential.

C. Force Field Parameters. The BK3 water force field is a four-site model which has a TIP4P-like structure. The OH bond length is 0.975 Å, and the bond angle is 104.52°. The van der Waals interaction site is assigned on the oxygen atom, and the oxygen−oxygen interactions are represented by the Buckingham potential.

$$u_{\mathrm{Buck},ij} = A\mathrm{e}^{-Br} - C/r^6 \tag{8}$$

The interaction parameters A and B of an unlike pair are calculated by the Kong combining rules,[60] and the interaction parameter C for unlike pairs is determined by the geometric combining rule. The electrostatic interactions are represented by three Gaussian charges:

$$u_{\mathrm{coul},ij} = \frac{1}{4\pi\epsilon_0}\sum_{a,b}\frac{q_{ia}q_{ib}}{|r_{ia}-r_{jb}|}\mathrm{erf}(\alpha_{iajb}|r_{ia}-r_{jb}|) \tag{9}$$

$$\alpha_{iajb} = \frac{1}{\sqrt{2\sigma_{ia}^2+2\sigma_{jb}^2}} \tag{10}$$

where σ_{ia} is the width of the charge distribution of Gaussian charge a of molecule i. Polarizability of the water molecule is represented by connecting the three Gaussian charges to the virtual site and hydrogen atoms with harmonic springs. Similar to the BK3 water model, the BK3 ion force fields also use the Buckingham potential and Gaussian charges to represent the van der Waals and electrostatic interactions, respectively. To account for the polarizability of ions, one Gaussian charge is connected to the ion atom with a harmonic spring. The parameters of the BK3 water model were obtained by fitting to the density of liquid water, density of hexagonal ice, dielectric constant, and minimum energy of the water dimer. Over the entire phase diagram, the BK3 water model gives reasonable estimates for many properties including densities, vapor pressures, vaporization enthalpies, viscosities, etc. The BK3 ion models are parametrized using salt solution and crystal properties at room temperature, including energy and structure of the ion−water cluster, solvation free energy, and crystalline solid density. Further details of the BK3 force fields can be found in the original publications.[38,39] The SWM4-NDP water force field also has a TIP4P-like structure, the OH bond length is 0.9572 Å, and the bond angle is 104.52°. A Lennard-Jones interaction site is assigned on the oxygen atom, and the polarizability is represented by a Drude particle of negative point charge attached to the oxygen atom. Further details of the SWM4-NDP and AH/SWM4-NDP models can be found in the original publications.[32,34,35]

Properties of the binary H_2O + NaCl mixture obtained from the polarizable BK3 models were compared with those obtained from nonpolarizable SPC/E+SD and SPC+SD models. SPC/E and SPC are widely used fixed-point-charge force fields for water, and they give reasonable estimates for densities and vapor pressures of pure water. The SD ion model,[11] which is compatible with SPC/E and SPC water models, is a simple nonpolarizable force field for ion. In ref 22, the SPC/E+SD and SPC+SD model combinations were found to give reasonable predictions for properties of the binary H_2O + NaCl mixture; however, Moučka et al.[16] found that the NaCl solubility was underestimated by this model combination. The parameters of the studied force fields are given in the Supporting Information.

III. RESULTS

Liquid densities, electrolyte and crystal chemical potentials of NaCl, salt solubilities, mean ionic activity coefficients, vapor pressures, interfacial tensions, and viscosities were obtained at 298.15, 373.15, and 473.15 K using the models and methods described in the previous section. Numerical data and their associated simulation uncertainties are listed in the Supporting Information. It was found that the model-predicted NaCl solubility is lower than the experimental value (as discussed in section B). Thus, for many of our simulations the solutions studied are supersaturated in salt, with the two-phase solution + crystal system having a lower free energy. However, crystal nucleation in simulations of supersaturated solutions is extremely difficult, as it has to occur by a homogeneous mechanism in a small system. We have confirmed that the simulations correspond to homogeneous solution conditions by calculating the pair correlation functions between positive and negative ions at the highest concentration studied (shown as a figure in Supporting Information).

A. Liquid Densities. Figure 1 shows the liquid densities of the binary H_2O + NaCl mixture at T = 298.15, 373.15, and 473.15 K and P = 100 bar, calculated using the BK3 models and the fixed-point-charge nonpolarizable SPC/E+SD models. This pressure is sufficiently high to ensure that the system is in the liquid phase at all temperatures and concentrations but also sufficiently near saturation conditions, given the incompressibility of the liquid solutions at conditions away from the solution's vapor−liquid critical point. The liquid densities for the SPC/E+SD models were obtained by isothermal−isobaric MD simulations in this work, and the details of the calculation were similar to the simulations using BK3 models. Both model combinations correctly predict the experimental trend, i.e., an increase of density with salt concentration, and the densities

DOI: 10.1021/acs.jctc.5b00421
J. Chem. Theory Comput. 2015, 11, 3802−3810

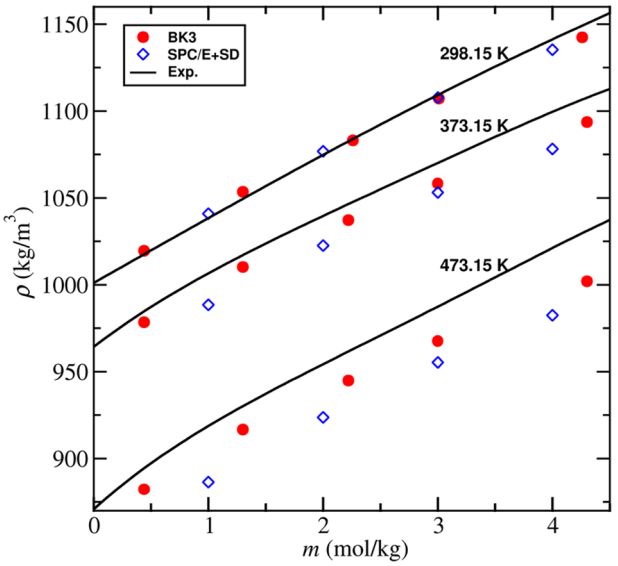

Figure 1. Liquid densities ρ (kg/m^3) for the system H_2O + NaCl at T = 298.15, 373.15, and 473.15 K and P = 100 bar versus NaCl molality, m, in mol NaCl/kg of H_2O. Solid lines are experimental data.[61] Red filled circles are for BK3 models. Blue open diamonds are for SPC/E +SD models. Statistical uncertainties are smaller than the symbol size.

calculated in this work are consistent with the results obtained by Moučka et al.[40] Compared with SPC/E+SD models, a better agreement with experimental data[61] can be achieved with the polarizable BK3 models, although slight underestimation of densities can be observed at 373.15 and 473.15 K.

B. Chemical Potentials and Mean Ionic Activity Coefficients. Figure 2 shows the electrolyte chemical potentials of the BK3 models as a function of salt concentration for the binary H_2O + NaCl mixture at T = 298.15 K, 373.15 K, and 473.15 K, and P = 1 bar (for systems at 298.15 and 373.15 K) and 15.5 bar (for systems at 473.15 K). These pressures are experimental saturated pressures of the H_2O + NaCl mixture (except 1 bar at 298.15 K), and properties of the mixture are mostly measured at these conditions.[62] The electrolyte chemical potentials of NaCl are represented by symbols and dashed lines, and dotted lines denote the crystal chemical potential of NaCl.

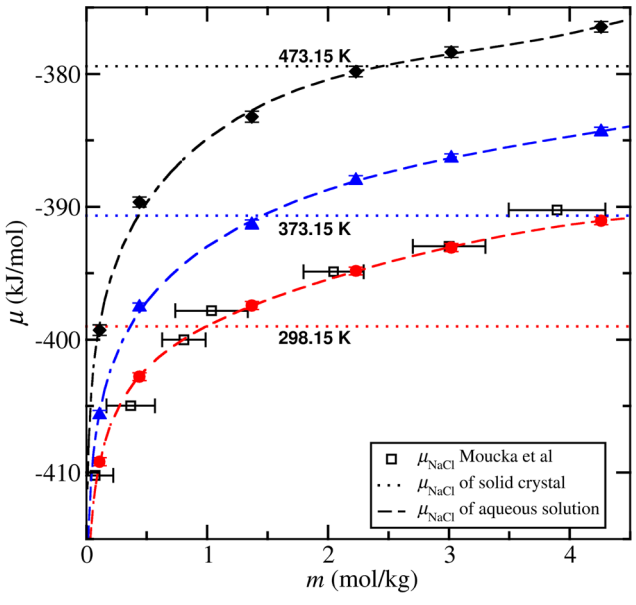

Figure 2. Electrolyte and crystal chemical potential μ (kJ/mol) of NaCl at 298.15 K and 1 bar, 373.15 K and 1 bar, and 473.15 K and 15.5 bar versus NaCl molality, m, in mol NaCl/kg of H_2O. Filled symbols are electrolyte chemical potentials of BK3 models obtained from MD simulations in the present work. Open squares are the electrolyte chemical potentials of BK3 models obtained from osmotic ensemble MC simualtions by Moučka et al.[40] Dotted lines denote the crystal chemical potentials of NaCl.

The electrolyte chemical potentials calculated at 298.15 K by MD simulations in the present work agree with the results obtained by Moučka et al. using osmotic ensemble MC simulations.[40] The crystal chemical potential at 298.15 K calculated from MC simulations in the present work is −399.0 ± 0.2 kJ/mol, which also agrees with the result obtained by Moučka et al.[40] (−399.2 ± 0.2 kJ/mol).

The salt solubilities for the BK3 models were calculated by finding the salt concentration where the electrolyte chemical potential equals the crystal chemical potential, which corresponds to the intersection of the dotted lines and dashed lines in Figure 2. Although the BK3 models give lower values at 298.15 K (0.99 ± 0.05 mol/kg) than experimental ones (6.1 mol/kg),[63] they predict correctly an increase in solubility with temperature (1.48 ± 0.06 mol/kg at 373.15 K, 2.51 ± 0.11 mol/kg at 473.15 K), which is consistent with the experimental observation (6.7 mol/kg at 373.15 K and 8.0 mol/kg at 473.15 K).[63]

Once the electrolyte chemical potentials have been obtained, the mean ionic activity coefficients can be calculated through eq 1. Figure 3 shows the mean ionic activity coefficients of NaCl as a function of solution concentration. The activity coefficient for SPC/E+SD models at 298.15 K are from ref 18, while the rest of the data were obtained in the present work (for convenience, all values are listed in Supporting Information). At 298.15 K, the activity coefficients predicted by the BK3 models agree well

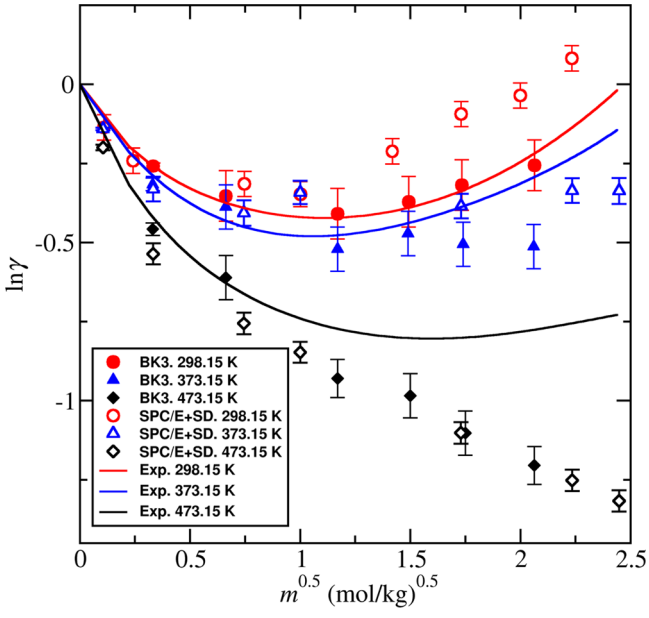

Figure 3. Mean ionic activity coefficient γ of NaCl at 298.15 K and 1 bar, 373.15 K and 1 bar, and 473.15 K and 15.5 bar versus NaCl molality in $m^{0.5}$. Solid lines are experimental data.[62] Filled symbols are for BK3 models. Open symbols are for SPC/E+SD models.

DOI: 10.1021/acs.jctc.5b00421
J. Chem. Theory Comput. 2015, 11, 3802−3810

with the experimental data.[62] Compared with the SPC/E+SD model, which significantly overestimates the activity coefficient at high salt concentrations, the effect of salt concentration on the activity coefficient is well captured by the BK3 models. In ref 18, the SPC/E+SD model was found to provide reasonable prediction for activity coefficients among a variety of nonpolarizable ion and water model combinations. Recenltly, we found that with simple nonpolarizable force field models, an accurate representation of activity coefficient at 298.15 K can only be obtained by the force field model proposed by Gee et al.,[64] whose parametrization included evaluation of the Kirkwood-Buff integrals at each salt concentration.[65,66] Therefore, we conclude that inclusion of polarizability in force field models plays an important role in the estimation of properties of electrolyte solutions.

Although the results from the BK3 models at 298.15 K are satisfactory, the model predictions start to deviate from experimental data as the temperature increases. At 373.15 K, experimental activity coefficients are similar to the corresponding values at 298.15 K. The polarizable BK3 models display a stronger temperature dependence and thus underestimate the activity coefficient at high salt concentration. This trend continues at higher temperatures, so the deviations at 473.15 K at high concentrations for the BK3 model are significant. A possible reason for this deficiency might be that the BK3 ion model was parametrized for solution properties at room temperature and that the temperature effect was not considered. At 373.15 K, with some deviations at high salt concentration, the activity coefficients predicted from nonpolarizable SPC/E+SD models are in better agreement with experimental data compared to the results at 298.15 K. Since the SPC/E+SD models significantly overestimate the activity coefficient at 298.15 K, the better representation of activity coefficients at 373.15 K indicates that the SPC/E+SD models have a stronger (thus, worse compared to experiment) temperature dependence than the BK3 model. At 473.15 K, SPC/E+SD and BK3 models give similar predictions, and both model combinations underestimate the mean activity coefficients at high salt concentration. It is worth noting that the SPC/E+SD models were parametrized at room temperature, so the better prediction of activity coefficients at higher temperature instead of 298.15 K could be a fortuitous error cancellation.

C. Vapor Pressures. Figure 4 shows the vapor pressures of the H_2O + NaCl mixture obtained from constant-volume Gibbs ensemble MC simulations using both the polarizable BK3 and nonpolarizable SPC+SD models (nonpolarizable results are from ref 22). We use here the SPC+SD models to compare against the BK3 models because the SPC/E model significantly underestimates the pure water vapor pressure.

As shown in the figure, both the BK3 and SPC+SD models follow the trend of the experimental data,[67] with both models slightly overestimating the vapor pressures. Since the vapor phase of the H_2O + NaCl mixture is relatively dilute, the vapor pressure of the mixture can also be determined from the water activity a_w and vapor pressure of pure water. The thermodynamic activity of water can be obtained from the mean ionic activity coefficients via the Gibbs−Duhem equation:

$$\ln a_w = 2M_w(-m - m\ln\gamma + \int_0^m \ln\gamma dm') \quad (11)$$

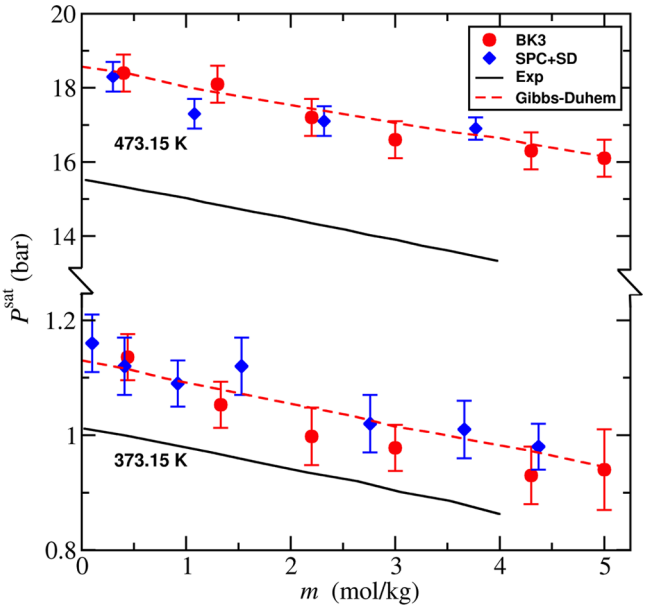

Figure 4. Vapor pressures P^{sat} (bar) for the system H_2O + NaCl at T = 373.15 K (bottom) and T = 473.15 K (top) versus NaCl molality, m, in mol NaCl/kg of H_2O. Solid black lines are experimental data.[67] Dashed lines are the vapor pressure of BK3 models calculated from the Gibbs−Duhem equation. Red filled circles are vapor pressures of BK3 models obtained from Gibbs ensemble MC simulations. Blue diamonds are vapor pressures of the SPC+SD model. The vapor pressures for the SPC + SD model are from ref 22.

where M_w is the molecular weight of water. The mean ionic activity coefficients obtained from the MD simulations in the previous section were fitted to the following equation:

$$\ln\gamma = \ln(10)\left(\frac{-A\sqrt{m}}{1 + B\sqrt{m}} + bm + Cm^2 + Dm^3\right) \quad (12)$$

where A is a constant (0.604 at 373.15 K for ϵ = 56 and 0.894 at 473.15 K for ϵ = 34) and B, b, C, and D are fitting parameters. Equation 12 with the fitting parameters was then numerically integrated according to eq 11 to calculate the water activity.[18] The pure water vapor pressure of the BK3 models was determined by extrapolating the vapor pressures of the binary mixture to zero salt concentration. As shown in Figure 4, the vapor pressures calculated from the water activity (Gibbs−Duhem equation) and vapor pressure of pure water are consistent with the results determined from Gibbs ensemble MC simulations. The vapor pressure for the polarizable AH/SWM4-NDP models[32,34] were also obtained in this work. However, the AH/SWM4-NDP models predict an increasing vapor pressure with salt concentration which is inconsistent with experimental data;[67] hence, the results for AH/SWM4-NDP models are not shown here but can be found in the Supporting Information.

D. Vapor−Liquid Interfacial Tensions and Viscosities. Figure 5 shows the prediction of the vapor−liquid interfacial tensions of a binary H_2O + NaCl mixture at T = 298.15, 373.15, and 473.15 K using the BK3 models; the interfacial tensions predicted by the nonpolarizable SPC/E+SD models (data from ref 22) are shown for comparison. From the results in Figure 5, the interfacial tensions are seen to increase with salt concentration, in agreement with the experimental trend.[68] The BK3 and SPC/E+SD models underestimate the interfacial tensions at 298.15 K, and similar underestimations can be

DOI: 10.1021/acs.jctc.5b00421
J. Chem. Theory Comput. 2015, 11, 3802−3810

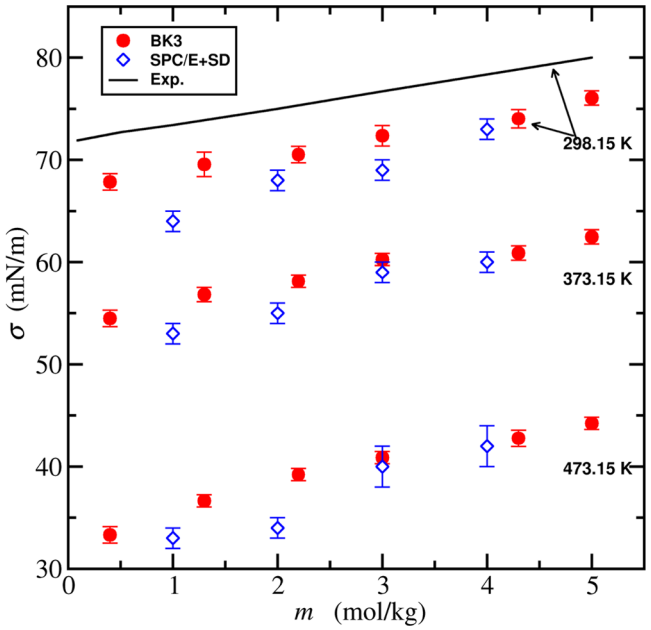

Figure 5. Vapor−liquid interfacial tensions σ (mN/m) for the system H_2O + NaCl at T = 298.15, 373.15, and 473.15 K versus NaCl molality, m, in mol NaCl/kg of H_2O. The black solid line corresponds to experimental data[68] at T = 298.15 K. Symbols are as described in Figure 1. Interfacial tensions data for SPC/E + SD models are from ref 22.

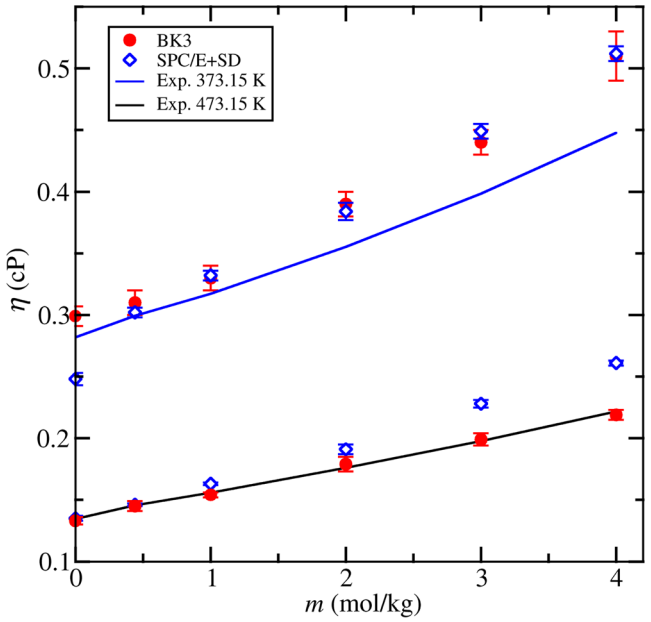

Figure 6. Shear viscosity η in cP for the system H_2O + NaCl at T = 373.15 and 473.15 K versus NaCl molality, m, in mol NaCl/kg of H_2O. Solid lines are experimental data.[67] Symbols are as described in Figure 1. Viscosity data for SPC/E+SD models are from ref 22.

expected at 373.15 and 473.15 K, though experimental data are not available at these temperatures. Compared to the nonpolarizable SPC/E+SD models, the BK3 models give a better prediction for interfacial tensions at low salt concentration, while the predictions from both model combinations at high salt concentration are similar. This indicates that the effect of salt concentration on interfacial properties is better estimated if the polarizability is included in the force fields.

Figure 6 shows the shear viscosity of the binary H_2O + NaCl mixture at 373.15 and 473.15 K predicted by BK3 and SPC/E +SD models (data from ref 22) as a function of the molal concentration of NaCl. At 373.15 K, BK3 models yield results similar to those of the SPC/E+SD models, and both model combinations overestimate the viscosity. At 473.15 K, the viscosities predicted by BK3 models are in excellent agreement with experimental data,[67] while the SPC/E+SD models still overestimate the viscosity.

IV. CONCLUSIONS

The binary H_2O + NaCl mixture was extensively studied in this work, by molecular simulations using the polarizable BK3 water and AH/BK3 ion force field models. Liquid densities, electrolyte and crystal chemical potentials, salt solubilities, mean ionic activity coefficients, vapor pressures, vapor−liquid interfacial tensions, and viscosities were obtained as functions of temperature, pressure, and salt concentration. The properties of the binary mixture predicted by the polarizable BK3 models were compared to results of SPC/E+SD and SPC+SD models, which are the most commonly used nonpolarizable force fields for the H_2O + NaCl mixture. For liquid densities, mean ionic activity coefficient, interfacial tensions, and viscosities, BK3 models give better predictions than the nonpolarizable SPC/E +SD models. For vapor pressures, the BK3 models yield predictions similar to those of the SPC+SD models. For salt solubility and the temperature effect on the mean ionic activity coefficients, the results of BK3 models are less satisfactory. It is concluded that the polarizable BK3 models can give reasonable estimates for most of the properties of interest simultaneously and that the inclusion of polarizability in the force field models improve the model performance for the H_2O + NaCl system. The unsatisfactory temperature effect of the BK3 models is arguably because the ion parameters were only adjusted to properties at ambient conditions. The performance of the BK3 force fields may be improved if properties at high temperatures can be included in the parametrization.

Although most of the properties of the binary H_2O + NaCl mixture are better represented by the polarizable BK3 models, the computational cost of the polarizable model on a single core is generally 5−10 times higher than that of the nonpolarizable models. While this factor may appear at first to be modest, the current version of GROMACS for the BK3 force fields runs only on a single core, while the simulation of nonpolarizable models can be efficiently scaled to more than 32 cores for the typical system sizes used in this work. The lack of scalable parallel codes makes the simulation of BK3 models much more expensive than the nonpolarizable force fields; this is an area in clear need of further software development.

■ ASSOCIATED CONTENT

Supporting Information

Force field parameters, numerical values of the densities, relative permittivities, chemical potentials, mean ionic activity coefficients, salt solubilities, vapor pressures, interfacial tensions, viscosities, their corresponding statistical uncertainties, vapor pressures of AH/SWM4-NDP models, and the $Na^+ - Cl^-$ pair correlation functions. The Supporting Information is available free of charge on the ACS Publications website at DOI: 10.1021/acs.jctc.5b00421.

DOI: 10.1021/acs.jctc.5b00421
J. Chem. Theory Comput. 2015, 11, 3802−3810

AUTHOR INFORMATION

Corresponding Author

*E-mail: azp@princeton.edu.

Funding

This publication was made possible by NPRP grant number 6-1157-2-471 from the Qatar National Research Fund (a member of Qatar Foundation). Additional support was provided by the Office of Basic Energy Sciences, U.S. Department of Energy, under Award DE-SC0002128, and by the Carbon Mitigation Initiative at Princeton University.

Notes

The statements made herein are solely the responsibility of the authors.

The authors declare no competing financial interest.

ACKNOWLEDGMENTS

We thank Dr. Peter Kiss, Dr. Andras Baranyai, and Dr. Marcelo Sega for providing computer source codes for the BK3 models and Professor Edward Maginn for access to early versions of the Cassandra codes.

REFERENCES

(1) Pitzer, K. S. *Activity Coefficient in Electrolyte Solutions*, 2nd ed.; CRC Press: Boca Raton, FL, 1991.

(2) Haghtalab, A.; Mazloumi, S. H. *Fluid Phase Equilib.* **2009**, *285*, 96−104.

(3) Lin, Y.; Thomsen, K.; Hemptinne, J. C. *AIChE J.* **2007**, *53*, 989−1005.

(4) Economou, I. G.; Peters, J.; de Swaan Arons, J. *J. Phys. Chem.* **1995**, *99*, 6182−6193.

(5) Galindo, A.; Gil-Villegas, A.; Jackson, G.; Burgess, A. N. *J. Phys. Chem. B* **1999**, *103*, 10272−10281.

(6) Held, C.; Sadowski, G. *Fluid Phase Equilib.* **2009**, *279*, 141−148.

(7) Hummer, G.; Soumpasis, D. M.; Neumann, M. *J. Phys.: Condens. Matter* **1994**, *6*, A141−A144.

(8) Brodholt, J. *Chem. Geol.* **1998**, *151*, 11−19.

(9) Berendsen, H. J. C.; Postma, J. P. M.; van Gunsteren, W. F.; Hermans, J. *Intermolecular Forces*; Pullman, B., Eds.; Reidel: Dordrecht, The Netherlands, 1981; pp 331−342.

(10) Berendsen, H. J. C.; Grigera, J. R.; Straatsma, T. P. *J. Phys. Chem.* **1987**, *91*, 6269−6271.

(11) Smith, D. E.; Dang, L. X. *J. Chem. Phys.* **1994**, *100*, 3757−3766.

(12) Lísal, M.; Smith, W. R.; Kolafa, J. *J. Phys. Chem. B* **2005**, *109*, 12956−12965.

(13) Moučka, F.; Lísal, M.; Škvor, J.; Jirsák, J.; Nezbeda, I.; Smith, W. R. *J. Phys. Chem. B* **2011**, *115*, 7849−7861.

(14) Moučka, F.; Lísal, M.; Smith, W. R. *J. Phys. Chem. B* **2012**, *116*, 5468−5478.

(15) Joung, I. S.; Cheatham, T. E. *J. Phys. Chem. B* **2008**, *112*, 9020−9041.

(16) Moučka, F.; Nezbeda, I.; Smith, W. R. *J. Chem. Phys.* **2013**, *138*, 154102−9.

(17) Moučka, F.; Nezbeda, I.; Smith, W. R. *J. Chem. Phys.* **2013**, *139*, 124505−7.

(18) Mester, Z.; Panagiotopoulos, A. Z. *J. Chem. Phys.* **2015**, *142*, 044507−10.

(19) Horn, H. W.; Swope, W. C.; Pitera, J. W.; Madura, J. D.; Dick, T. J.; Hura, G. L.; Head-Gordon, T. *J. Chem. Phys.* **2004**, *120*, 9665−9678.

(20) Errington, J. R.; Panagiotopoulos, A. Z. *J. Phys. Chem. B* **1998**, *102*, 7470−7475.

(21) Fumi, F. G.; Tosi, P. *J. Phys. Chem. Solids* **1964**, *25*, 31−43.

(22) Orozco, G. A.; Moultos, O. A.; Jiang, H.; Economou, I. G.; Panagiotopoulos, A. Z. *J. Chem. Phys.* **2014**, *141*, 234507−8.

(23) López-Lemus, J.; Chapela, G.; Alejandre, J. *J. Chem. Phys.* **2008**, *128*, 174703.

(24) Rick, S. W.; Stuart, S. J.; Berne, B. J. *J. Chem. Phys.* **1994**, *101*, 6141−6156.

(25) Jorgensen, W. L.; Madura, J. D. *Mol. Phys.* **1985**, *56*, 1381−1392.

(26) Ren, P. Y.; Ponder, J. W. *J. Phys. Chem. B* **2003**, *107*, 5933−5947.

(27) Ponder, J. W.; Wu, C.; Ren, P.; Pande, V. S.; Chodera, J. D.; Schnieders, M. J.; Haque, I.; Mobley, D. L.; Lambrecht, D. S.; DiStasio, R. A., Jr; Head-Gordon, M.; Clark, G. N. I.; Johnson, M. E.; Head-Gordon, T. *J. Phys. Chem. B* **2010**, *114*, 2549−2564.

(28) Chipman, D. M. *J. Phys. Chem. B* **2013**, *117*, 5148−5155.

(29) Paricaud, P.; Predota, M.; Chialvo, A. A.; Cummings, P. T. *J. Chem. Phys.* **2005**, *122*, 244511−14.

(30) Chialvo, A. A.; Moučka, F.; Vlcek, L.; Nezbeda, I. *J. Phys. Chem. B* **2015**, *119*, 5010−5019.

(31) Yu, H.; van Gunsteren, W. F. *J. Chem. Phys.* **2004**, *121*, 9549−9564.

(32) Lamoureux, G.; Harder, E.; Vorobyov, I. V.; Roux, B.; MacKerell, A. D., Jr *Chem. Phys. Lett.* **2006**, *418*, 245−249.

(33) Yu, W.; Lopes, P. E. M.; Roux, B.; MacKerell, A. D., Jr *J. Chem. Phys.* **2013**, *138*, 034508.

(34) Lamoureux, G.; Roux, B. *J. Phys. Chem. B* **2006**, *110*, 3308−3322.

(35) Yu, H.; Whitfield, T. W.; Harder, E.; Lamoureux, G.; Vorobyov, I.; Anisimov, V. M.; MacKerell, A. D., Jr; Roux, B. *J. Chem. Theory Comput.* **2010**, *6*, 774−786.

(36) Neyt, J. C.; Wender, A.; Lachet, V.; Ghoufi, A.; Malfreyt, P. *Phys. Chem. Chem. Phys.* **2013**, *15*, 11679−90.

(37) Moučka, F.; Nezbeda, I.; Smith, W. R. *Mol. Simul.* **2013**, *39*, 1125−1134.

(38) Kiss, P. T.; Baranyai, A. *J. Chem. Phys.* **2013**, *138*, 204507−17.

(39) Kiss, P. T.; Baranyai, A. *J. Chem. Phys.* **2014**, *141*, 114501−15.

(40) Moučka, F.; Nezbeda, I.; Smith, W. R. *J. Chem. Theory Comput.* **2015**, *11*, 1756−1764.

(41) Hess, B.; Kutzner, C.; van der Spoel, D.; Lindahl, E. *J. Chem. Theory Comput.* **2008**, *4*, 435−447.

(42) Kiss, P. T.; Sega, M.; Baranyai, A. *J. Chem. Theory. Comput* **2014**, *10*, 5513−5519 The modified GROMACS package is available at http://marcello-sega.github.io/gromacs/.

(43) Nosé, S. *Mol. Phys.* **1984**, *52*, 255−268.

(44) Parrinello, M.; Rahman, A. *J. Appl. Phys.* **1981**, *52*, 7182−7190.

(45) Kolafa, J. *J. Comput. Chem.* **2004**, *25*, 335−342.

(46) Bennett, C. H. *J. Comput. Phys.* **1976**, *22*, 245−268.

(47) Paliwal, H.; Shirts, M. *J. Chem. Theory Comput.* **2011**, *7*, 4115−4134.

(48) Davies, C. W. *Ion Association*; Butterworths: Washington, DC, 1962.

(49) Chase, M. W. *NIST-JANAF Thermochemical Tables*, Fourth Edition, Monograph 9, 1998; p 836.

(50) Rowlinson, J. S.; Widom, B. *Molecular Theory of Capillarity*; Clarendon Press: Oxford, 1982.

(51) Liu, Y.; Lafitte, T.; Panagiotopoulos, A. Z.; Debenedetti, P. G. *AIChE J.* **2013**, *59*, 3514−22.

(52) Sadus, R. J. *Molecular Simulation of Fluids: Theory, Algorithms and Object-Orientation*; Elsevier: Amsterdam, 1999.

(53) Shah, J.; Maginn, E. *J. Chem. Phys.* **2011**, *135*, 134121−11.

(54) Panagiotopoulos, A. Z. *Mol. Phys.* **1987**, *61*, 813−826.

(55) Panagiotopoulos, A. Z.; Quirke, N.; Stapleton, M.; Tildesley, D. J. *Mol. Phys.* **1988**, *63*, 527−545.

(56) Baranyai, A.; Kiss, P. T. *J. Chem. Phys.* **2010**, *133*, 144109−10.

(57) Siepmann, I. J. *Mol. Phys.* **1990**, *70*, 1145−1158.

(58) Frenkel, D.; Smit, B. *Understanding Molecular Simulation*; Academic Press: San Diego, CA, 2002.

(59) Aragones, J. L.; Valeriani, C.; Vega, C. *J. Chem. Phys.* **2012**, *137*, 146101−2.

(60) Kong, C. L.; Chakrabarty, M. R. *J. Phys. Chem.* **1973**, *77*, 2668−2670.

(61) Potter, R. W.; Brown, D. L. The Volumetric Properties of Aqueous Sodium Chloride Solutions from 0 to 500 C at Pressures up

DOI: 10.1021/acs.jctc.5b00421
J. Chem. Theory Comput. 2015, 11, 3802−3810

to 2000 bar Based on a Regression of Available Data in Literature; *Geological Survey Bulletin* 1421-C, United States Government Printing Office: Washington, D. C., 1977.
(62) Pitzer, K. S.; Peiper, J. C.; Busey, R. H. *J. Phys. Chem. Ref. Data* **1984**, *13*, 1−102.
(63) Cohen, P. *ASME Handbook on Water Technology for Thermal Power Systems*; ASME: New York, 1989.
(64) Gee, M. B.; Cox, N. R.; Jiao, Y.; Bentenitis, N.; Weerasinghe, S.; Smith, P. E. *J. Chem. Theory Comput.* **2011**, *7*, 1369−1380.
(65) Weerasinghe, S.; Smith, P. E. *J. Phys. Chem. B* **2003**, *107*, 3891−3898.
(66) Mester, Z.; Panagiotopoulos, A. Z. *J. Chem. Phys.* 2015, *143*; DOI: 10.1063/1.4926840.
(67) Phillips, S. L.; Igbene, A.; Fair, J. A.; Ozbek, H.; Tavana, H. *A Technical Databook for Geothermal Energy Utilization*; Lawrence Berkeley Laboratory, UC Berkeley: Berkeley, CA, 1981.
(68) Abramzon, A. A.; Gauberk, R. D. *Zh. Prek. Khim.* **1993**, *66*, 1428.

DOI: 10.1021/acs.jctc.5b00421
J. Chem. Theory Comput. 2015, 11, 3802−3810